

Article

# An Improved Sorting Algorithm for Periodic PRI Signals Based on Congruence Transform

Huixu Dong \*, Yuanzheng Ge, Rui Zhou and Hongyan Wang

Air Force Aviation University, Changchun 130022, China; ge\_yuanzheng@163.com (Y.G.); rui\_zhoucheif@126.com (R.Z.)

\* Correspondence: me\_isdx@163.com

**Abstract:** Recently, a signal sorting algorithm based on the congruence transform has been proposed, which is effective in dealing with the staggered Pulse Repetition Interval (PRI) signals. It can effectively sort the staggered PRI signals and obtain the sub-PRI sequence directly without sub-PRI ranking, and it is less affected by interfered pulses and pulse loss. Nevertheless, we find that the algorithm causes pseudo-peaks in the remainder histogram when sorting signals such as sliding PRI, sinusoidal PRI, etc. (collectively referred to as periodic PRI signal in this paper) and pseudo-peaks will cause errors in signal sorting. To solve the issue of pseudo-peaks when sorting periodic PRI signals, an improved sorting algorithm based on congruence transform is proposed. According to the analysis of the congruence characteristics of the periodic PRI signal, a novel method is proposed to identify pseudo-peaks based on the histogram peak amplitude and symmetric difference set. The signal sorting algorithm based on congruence transform is improved to achieve a good sorting effect on periodic PRI signals. Simulation experiments demonstrate that the novel algorithm can effectively sort periodic PRI signals and improve  $P_{recall}$ ,  $P_d$ , and  $P_f$  by 6.9%, 5.1%, and 3.2%, respectively, compared to the typical similar algorithms.

**Keywords:** periodic PRI signals; improved algorithm; signal sorting; congruence transform



**Citation:** Dong, H.; Ge, Y.; Zhou, R.; Wang, H. An Improved Sorting Algorithm for Periodic PRI Signals Based on Congruence Transform. *Symmetry* **2024**, *16*, 398. <https://doi.org/10.3390/sym16040398>

Academic Editors: Jeng-Shyang Pan, Rumen Mironov and Roumiana Kountcheva

Received: 28 January 2024

Revised: 7 March 2024

Accepted: 19 March 2024

Published: 28 March 2024



**Copyright:** © 2024 by the authors. Licensee MDPI, Basel, Switzerland. This article is an open access article distributed under the terms and conditions of the Creative Commons Attribution (CC BY) license (<https://creativecommons.org/licenses/by/4.0/>).

## 1. Introduction

In electronic support system signal processing, radar signal sorting is a critical task. The purpose of signal sorting is to distinguish different radar emitter signals. This is essential for extracting features and identifying radar emitter signals [1–5]. Generally, there are two types of radar signal sorting methods [6,7]: one involves pre-sorting algorithms based on parameter correlation, and the other focuses on PRI sorting methods based on the correlation of Time Of Arrival (TOA) between pulses. The process of de-interleaving pulse sequences based on TOA and identifying modulation types based on PRI can be used to sort multiple interleaved radar emitter signals by utilizing the relevance from the same emitter. This is an effective method for sorting radar emitter signals.

Classical PRI sorting algorithms include the cumulative difference histogram (CDIF) algorithm [8] and the CDIF-based sequential difference histogram (SDIF) algorithm [9]. The two algorithms are easy to implement and have high sorting efficiency. However, they cannot suppress harmonics generated by pulse loss and have poor sorting ability for complex modulation signals, such as staggered PRI and sliding PRI. To overcome the problem of pulse loss, Xie, M. proposed a first-order difference curve based on a sorted TOA difference sequence algorithm (FDC-DTOA) which can suppress harmonics generated by pulse loss. But it has poor sorting ability for complex modulation signals [10]. For the case of missing and short observations, Guo, Q. proposed a radar pulse train de-interleaving method which is particularly suitable for the interleaving of the short and highly interleaved missing pulse train in complex electromagnetic environments. However, this method cannot sort periodic PRI signals and the complexity of the algorithm is high [11]. The PRI transform algorithm

has a good capability for suppressing harmonics, but it cannot sort signals with staggered PRI, sliding PRI, or other complex modulation types [12]. To address the issue of the poor sorting capability of the PRI transform algorithm for PRI modulated signals, Liu and Kocamis combined the PRI transform algorithm with the sequence extraction algorithm to estimate the frame period of staggered PRI signals. This allows for PRI assessment of the environment after extracting sub-PRI sequences to sort staggered PRI signals [13,14]. Liu, Z.M. proposed a frequent term expansion algorithm, which can effectively identify staggered PRI signals. But it cannot sort interleaved pulses [15]. Kang, S.Q. introduced a measure of interest degree for association patterns based on a frequent term expansion algorithm. This measure can be used to sort and identify staggered PRI signals in interleaved pulse sequences. However, the stop condition of the algorithm is too complex, making it difficult to implement in engineering [16]. Wang, J.L. proposed a method to establish a pulse interval distribution matrix by connecting pulse pair intervals and individual pulses. This achieves simultaneous harmonic suppression and frame period extraction, based on the extended correlation method and eigenvector method [17]. However, this method requires the ranking of the staggered PRI signal sub-sequence. In [18,19], a correlation matching algorithm is proposed for signal detection and parameter extraction of staggered PRI signals. The algorithm operates in an orthogonal Ramanujan subspace with fewer non-zero elements for reducing computational complexity. However, it has limited adaptability to sinusoidal PRI and sliding PRI. In [20], a framework of fuse multiple existing pulse train de-interleaved methods is proposed, which can be used to separate individual pulse trains included in the received pulse trains. It has the best robustness for missing pulse and PRI jitter, and can effectively de-interleave the received pulse train with PRI stagger and jittered PRI. Dong, H. proposed a PRI sorting algorithm based on congruence transform by utilizing the periodicity of PRI, which can sort fixed PRI and staggered PRI signals effectively [21]. It has good anti-pulse loss and anti-interference properties without sub-PRIs ranking, but cannot suppress the residual histogram pseudo-peaks when sorting periodic PRI signals.

To deal with the pseudo-peaks' problems in the signal sorting of the periodic PRI, an improved signal sorting algorithm based on the congruence transform is proposed. Firstly, from the point of view of periodicity, this paper establishes a periodic PRI signal model and analyses the characteristics of the signal. Secondly, according to the analysis of the congruence characteristics of the periodic PRI signal, a method is proposed to identify pseudo-peaks based on the histogram peak amplitude and symmetric difference set, and the specific flow of the improved algorithm is given. Finally, the validity of the proposed algorithm is verified by simulation experiments.

## 2. Model and Analysis

### 2.1. Signal Model of Periodic PRI

When only TOA is considered, the pulse trains detected by the receiver can be written as

$$P(t) = \sum_{n=1}^N \delta(t - t_n) \quad (1)$$

where  $\delta(t)$  is the impulse function,  $t_n$  is the TOA of the  $n$ th pulse, and  $N$  is the number of pulses. The change pattern of  $t_n$  reflects the type of modulation of the PRI.

When  $t_n$  follows a sawtooth wave, sinusoidal or linear, the PRI modulation type of the pulse sequence could be slip, sinusoidal, or another modulation type [22], as shown in Figure 1.

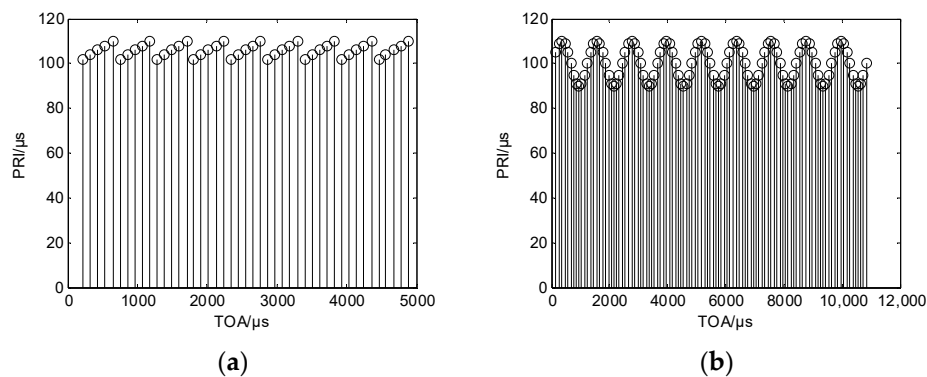


Figure 1. PRI modulation signal: (a) sliding PRI signal sequence; (b) sinusoidal PRI signal sequence.

Similar to the staggered PRI signal model mentioned in Dong, H.’s work [21], the pulse trains with sliding PRI, sinusoidal PRI, and other PRI modulation (repeats with the frame period  $T_z$ ) can be regarded as a superposition of the fixed PRI pulse sequence with a different start time, as shown in Figure 2.

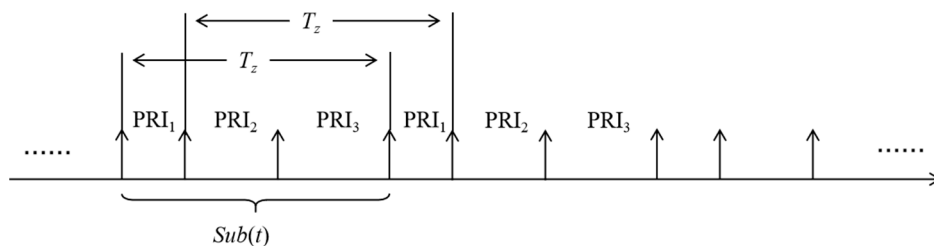


Figure 2. Periodic PRI signal pulse sequence.

The periodic PRI signal model is expressed as

$$\begin{cases} P(t) = \sum_{k=1}^K \sum_{n_k=1}^{N_k} \delta(t - t_k - n_k T_z) \quad n_k = 1, 2, \dots, N_k \\ T_z = \sum_{k=1}^{K-1} PRI_k = \sum_{k=1}^{K-1} (t_{k+1} - t_k) \\ Sub(t) = \sum_{k=1}^K \delta(t - t_k) \end{cases} \quad (2)$$

where  $t_k$  is the TOA of the pulse sequence within the frame period,  $Sub(t)$  is the sub-pulse sequence,  $T_z$  is the frame period, and  $K > 1$ .

### 2.2. Analysis of Periodic PRI Signal Based on Congruence Transform

From Equation (2), the periodic PRI signal can be regarded as the superposition of multiple fixed PRI pulse sequences with period  $T_z$ ; then, the TOA of  $k$ th fixed PRI pulse sequences can be written as

$$TOA_k(n) = t_k + nT_z, \quad n = 1, 2, 3 \dots \quad (3)$$

If we calculate the congruence transform of the TOA for periodic PRI signals modulo positive integer  $T_0$ , then we obtain

$$\text{mod}[TOA_k(n), T_0] = \text{mod}[t_k, T_0] + \text{mod}[nT_z, T_0] \quad (4)$$

where  $\text{mod}[\cdot]$  denotes the remainder operation.

### 2.2.1. Congruence Transform of Periodic PRI Signal

When  $T_0 = T_z$ , Equation (4) can be simplified as

$$\text{mod}[TOA_k(n), T_0] = \text{mod}[t_k, T_0] \quad (5)$$

Equation (5) shows that the TOA of all pulses has the same remainder. The remainder is related only to the TOA of the first pulse  $t_k$ , and is independent of the pulse index number  $n$ , and this process is called congruent transform in [21].

Then, congruence transform is conducted on the periodic PRI signals such as sliding PRI with PRIs as  $\{\text{PRI} \mid \text{PRI} = 100 + 2n, n = 1, 2, \dots, 5\}$  and sinusoidal PRI with PRIs as  $\{\text{PRI} \mid \text{PRI} = 100 + 10\sin(2\pi n/12), n = 1, 2, \dots, 12\}$ . The results we obtained are shown in Figure 3.

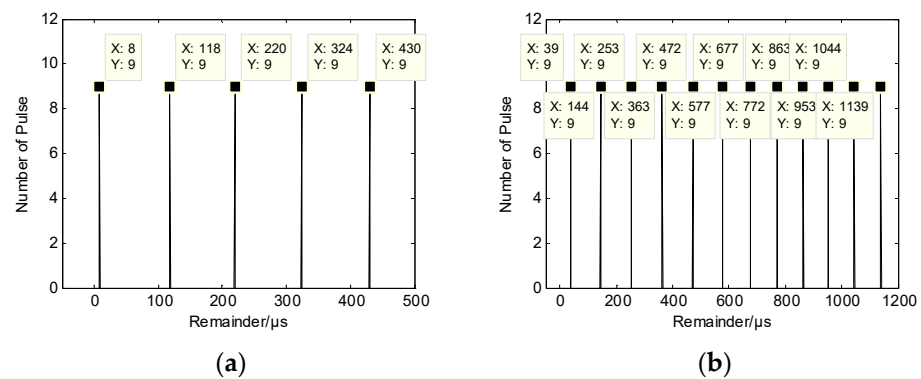


**Figure 3.** Histogram of remainder for different PRI modulation types: (a) remainder histogram of sliding PRI; (b) remainder histogram of sinusoidal PRI.

From Figure 3a, it can be seen that the periodic PRI signals after the congruence transform are gathered at five points,  $8 \mu\text{s}$ ,  $118 \mu\text{s}$ ,  $220 \mu\text{s}$ ,  $324 \mu\text{s}$ , and  $430 \mu\text{s}$ , with a frame period of  $530 \mu\text{s}$ .  $\{8 \mu\text{s}, 118 \mu\text{s}, 220 \mu\text{s}, 324 \mu\text{s}, 430 \mu\text{s}\}$  are exactly the  $t_k$  of the pulse sequence. Thus, we can obtain the PRIs as  $\{102 \mu\text{s}, 104 \mu\text{s}, 106 \mu\text{s}, 108 \mu\text{s}\}$  by adjacent subtraction operation with  $\{8 \mu\text{s}, 118 \mu\text{s}, 220 \mu\text{s}, 324 \mu\text{s}, 430 \mu\text{s}\}$ . Then, another PRI  $110 \mu\text{s}$  can be obtained by subtraction operation with  $\{102 \mu\text{s}, 104 \mu\text{s}, 106 \mu\text{s}, 108 \mu\text{s}\}$  and  $530 \mu\text{s}$ .  $\{102 \mu\text{s}, 104 \mu\text{s}, 106 \mu\text{s}, 108 \mu\text{s}, 110 \mu\text{s}\}$  are the sub-PRIs of the sliding PRI signal. Similarly, the same conclusion can be drawn from Figure 3b in the case of sinusoidal PRI signals. It can be concluded that the staggered PRI signal sequence undergoes a congruent transform modulo the frame period gathered in  $\text{mod}(t_k, T_z)$ .

When  $T_0 \neq T_z$ , if  $T_0 \neq mT_z$  and  $T_z \neq mT_0$ , Equation (4) can be written as

$$\begin{cases} \text{mod}[TOA_k(n), T_0] = \text{mod}[t_k, T_0] + \text{mod}[n\Delta T, T_0] \\ \Delta T = \text{mod}[T_z, T_0] \end{cases} \quad (6)$$

It can be seen that the remainders of the TOA of the pulse sequence are not equal, and they are related to the pulse number  $n$ , i.e., as  $n$  increases, the remainder increases.

### 2.2.2. Pseudo-Peak Analysis of the Congruence Transform

When  $T_0 \neq T_z$ , if  $T_0 = mT_z$  or  $T_z = mT_0$ ,  $m$  is an integer greater than 1. Under the condition of  $T_0 = mT_z$ , the value of  $T_0$  is  $m$  times the actual frame period  $T_z$ , and then Equation (4) is converted to

$$\text{mod}[TOA_k(n), T_0] = \text{mod}[t_k, mT_z] + \text{mod}[nT_z, mT_z] \quad (7)$$

The remainder of the signal sequence is not only related to  $t_k$ , but also related to the value of  $m$ . The number of peaks in the congruence transform results is  $m$  times the number in Figure 3.

The congruence transform is conducted on the same data of Figure 3 with modulo positive integer  $T_0 = mT_z$  ( $m = 2$ ). The results are shown in Figure 4.

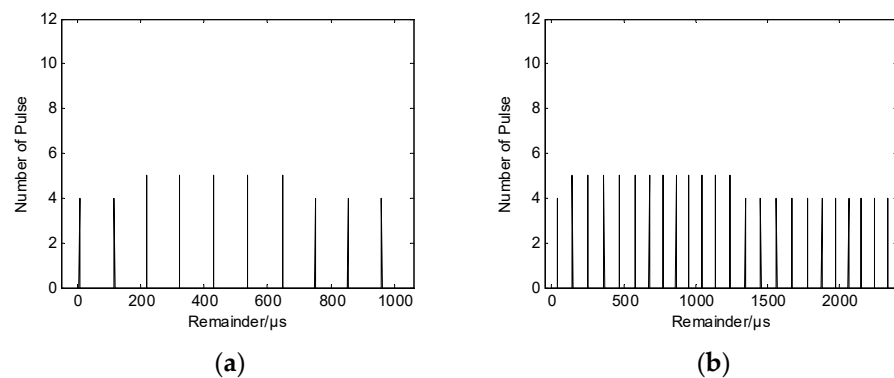


**Figure 4.** Histogram of remainder for different PRI modulation types: (a) remainder histogram of sliding PRI with a frame period of 1060  $\mu\text{s}$ ; (b) remainder histogram of sinusoidal PRI with a frame period of 2400  $\mu\text{s}$ .

In Figure 4a, the periodic PRI signals after the congruence transform are gathered at ten points, 8  $\mu\text{s}$ , 118  $\mu\text{s}$ , 220  $\mu\text{s}$ , 324  $\mu\text{s}$ , 430  $\mu\text{s}$ , 538  $\mu\text{s}$ , 648  $\mu\text{s}$ , 750  $\mu\text{s}$ , 854  $\mu\text{s}$ , and 960  $\mu\text{s}$ , with a frame period of 1060  $\mu\text{s}$ . As shown in Figure 4a, when  $T_0 = mT_z$ , the congruence transform produces a lot of pseudo-peaks. Similarly, the same conclusion can be drawn from Figure 3b in the case of sinusoidal PRI signals.

When  $T_z = mT_0$ , the value of  $T_0$  is taken as  $1/m$  of the frame period, and Equation (4) is converted to

$$\begin{aligned} \text{mod}[TOA_k(n), T_0] &= \text{mod}\left[t_k, \frac{T_z}{m}\right] + \text{mod}\left[nT_z, \frac{T_z}{m}\right] \\ &= \text{mod}\left[t_k, \frac{T_z}{m}\right] \end{aligned} \quad (8)$$

Under this condition, the congruence transform is conducted on the same data of Figure 3 modulo positive integer  $T_0 = mT_z$  ( $m = 2$ ); the results are shown in Figure 5.

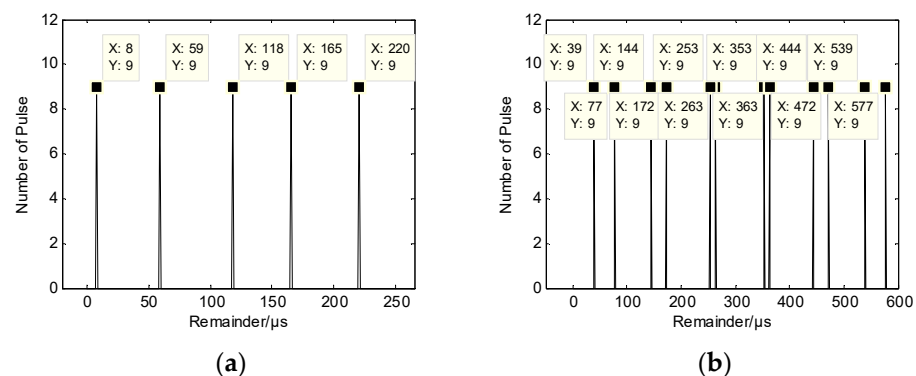


**Figure 5.** Histogram of remainder for different PRI modulation types: (a) remainder histogram of sliding PRI with a frame period of 265  $\mu\text{s}$ ; (b) remainder histogram of sinusoidal PRI with a frame period of 600  $\mu\text{s}$ .

In Figure 5a, the periodic PRI signals after the congruence transform are gathered at ten points, 8  $\mu\text{s}$ , 59  $\mu\text{s}$ , 118  $\mu\text{s}$ , 165  $\mu\text{s}$ , and 220  $\mu\text{s}$ , with a frame period of 265  $\mu\text{s}$ . We can obtain the sub-PRI of the sliding PRI signal {51  $\mu\text{s}$ , 59  $\mu\text{s}$ , 47  $\mu\text{s}$ , 35  $\mu\text{s}$ , 45  $\mu\text{s}$ } with the same calculations as in Section 2.2.1. Sub-PRI {51  $\mu\text{s}$ , 59  $\mu\text{s}$ , 47  $\mu\text{s}$ , 35  $\mu\text{s}$ , 45  $\mu\text{s}$ } are not equal to the true sub-PRI {102  $\mu\text{s}$ , 104  $\mu\text{s}$ , 106  $\mu\text{s}$ , 108  $\mu\text{s}$ , 110  $\mu\text{s}$ }. As shown in Figure 5a, when

$T_0 = T_z/m$  ( $m = 2$ ), peaks of the congruence transform are all pseudo-peaks. Similarly, the same conclusion can be drawn from Figure 5b in the case of sinusoidal PRI signals.

To sum up, three conclusions can be drawn as follows. If  $T_0 = T_z$ , the remainder of the periodic PRI sequence is a fixed value, and the number of pulses with the same remainder satisfies the Formula (5), and the position of the remainder histogram peaks can reflect the value and order of the sub-PRI; if  $T_0 \neq T_z$ ,  $T_0 = mT_z$  or  $T_z = mT_0$ , ( $m$  is an integer greater than 1), the histogram has several peaks, but the size, number, and position of peaks will change, which cannot reflect the value and order of sub-PRI; when  $T_0 \neq T_z$ ,  $T_0 \neq mT_z$  or  $T_z \neq mT_0$ , the remainders of the pulse sequence are not equal and are related to the pulse order number  $n$ , and there are no more peaks in the histogram.

### 3. Periodic PRI Signal Sorting

#### 3.1. Principle of Periodic PRI Signal Sorting

For periodic PRI signals, the change rule of the sub-PRI is different from that of the staggered PRI signals, which will have an impact on the design of the signal sorting algorithm. Since the change rule of the sub-PRI can be expressed as a certain function, the frame period may be a multiple of the sub-PRI, i.e.,

$$T_z = m \sum_{k=1}^L \text{PRI}_k, L < K \quad (9)$$

where  $m$ ,  $L$ , and  $K$  are positive integers and  $T_z$  is the frame period. We can conclude that the congruence transform produces a lot of pseudo-peaks based on the analysis in Section 2.2.2. Then, the periodic PRI signal is truncated into some sequences using the baseline algorithm in [21], which will cause errors in the signal sorting. Therefore, this paper proposes an improved sorting algorithm for periodic PRI signals based on congruence transform.

From the analysis of Equation (5) in Section 2.2.1, the pulse number with the same remainder  $N_{m0}$  in congruence transform is as follows:

$$N_{m0} = \frac{(TOA_{end} - TOA_{begin})}{T_z} + 1 \quad (10)$$

where  $TOA_{begin}$  and  $TOA_{end}$  are the first TOA and the last TOA of the pulse sequence, respectively.

Considering the pulse loss condition, the pulse number with the same remainder  $N_{m0}$  satisfies

$$N_{m0} < \frac{(TOA_{end} - TOA_{begin})}{T_z} + 1 \quad (11)$$

When  $T_0 = mT_z$ , the value of  $T_0$  is  $m$  times the actual frame period  $T_z$ . The remainder of the signal sequence is not only related to  $t_k$ , but also related to the value of  $m$ . The number of pulses with the same remainder  $N_{m0}$  satisfies

$$N_{m0} \leq \frac{(TOA_{end} - TOA_{begin})}{mT_z} + 1 \quad (12)$$

When  $T_0 = T_z/m$ , the value of  $T_0$  is taken as  $1/m$  of the frame period, and the number of congruent pulses  $N_{m0}$  satisfies

$$N_{m0} \leq \frac{(TOA_{end} - TOA_{begin})}{mT_0} + 1 \quad (13)$$

i.e.,

$$N_{m0} \leq \frac{(TOA_{end} - TOA_{begin})}{T_z} + 1 \quad (14)$$

Based on (10), (12) and (14), pseudo-peaks in the  $T_0 = mT_z$  condition can be identified and eliminated.

**Definition:** Symmetric Difference Set. The symmetric difference set of A and B is defined as the set of all elements of set A and set B. They are not part of  $A \cap B$ , and are denoted as  $A \Delta B$ ,

$$A \Delta B = \{x | x \in A \cup B, x \notin A \cap B\} \quad (15)$$

From the analysis in Section 2, it can be seen that the sub-PRIs of the periodic PRI signals can be directly computed from the result of the congruence transformation at  $T_0 = T_z$ , denoted as set  $\Theta$ . Meanwhile, the sub-PRIs of the periodic PRI signals can also be estimated from the extraction sequence, denoted as set  $\Gamma$ . Obviously, when  $T_0 = T_z$ , then  $\Theta \Delta \Gamma = \emptyset$ ; when  $T_0 = T_z/m$ , then  $\Theta \Delta \Gamma \neq \emptyset$ . Therefore, pseudo-peaks in the  $T_0 = T_z/m$  condition can be identified and eliminated.

### 3.2. Flow of Periodic PRI Signal Sorting Algorithm

According to the analysis above, we propose an improved sorting algorithm of periodic PRI signals based on congruence transform, and the algorithm flow chart is shown in Figure 6.

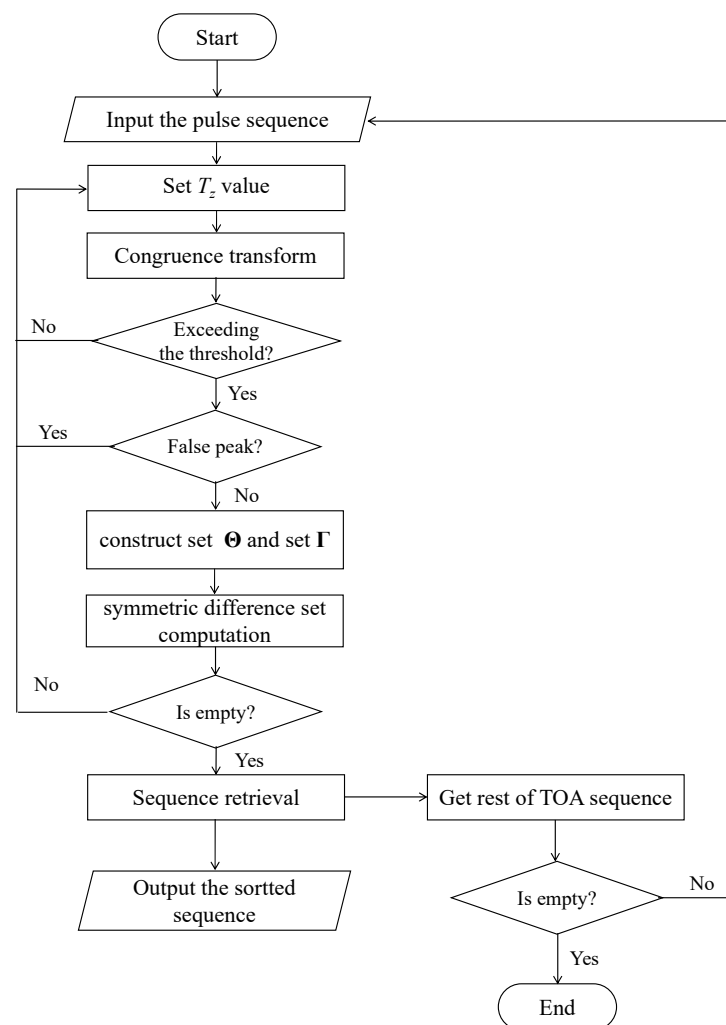


**Figure 6.** Flow of signal sorting algorithm.

The specific steps are as follows:

Step 1: Input the TOA sequence of the signal to be sorted;

Step 2: Set the value range of the frame period as  $[T_{\min}, T_{\max}]$ , the search step  $\Delta t$ , and the frame period  $T_z = T_{\min} + (i - 1) \Delta t$  for the  $i$ th calculation;

Step 3: Calculate the remainder of the signal sequence modulo positive integer  $T_z$  to obtain the set  $\Phi$  which is composed of the remainders of the pulse sequence, and calculate the vector  $\mathbf{a}$  corresponding to the histogram of the set  $\Phi$  which is composed of the remainders of the pulse sequence;

Step 4: Set a histogram detection threshold  $\varepsilon$ , and when the amplitude of vector  $\mathbf{a}$  is less than  $\varepsilon$ , make the amplitude zero, then obtain a detected histogram vector  $\mathbf{b}$ ;

Step 5: The non-zero values in vector  $\mathbf{b}$  are judged by using the conditions of Equations (10), (12) and (14) to remove the pseudo-peaks and obtain vector  $\mathbf{c}$ ;

Step 6: If there is a non-zero value in  $\mathbf{c}$ , determine whether the frame period  $T_z$  exists, group the pulse sequences with the same remainder together according to the histogram, and complete the signal sorting. And the set  $\Gamma$  is constructed. Extract the remainder vector  $\mathbf{d}$  corresponding to the peak of the sequence remainder histogram, and find the difference in the neighboring elements of vector  $\mathbf{d}$  to obtain the sub-PRI. And the set  $\Theta$  is constructed;

Step 7: Compute the symmetric difference between set A and set B;

Step 8: if  $\Theta \Delta \Gamma = \emptyset$ , then extract the remainder vector  $\mathbf{d}$  corresponding to the peak of the sequence remainder histogram and the rest of the pulse sequences are used as new inputs, then go to step 1; otherwise, go to step 2;

Step 9: Output sequence of the signal has been sorted.

### 3.3. Computational Complexity Analysis

According to the steps above, the proposed algorithm needs to search in the range of  $[T_{\min}, T_{\max}]$  during the operation, and the search step is  $\Delta t$ . The algorithm needs to be performed  $P$  times of remainder histogram operations, with  $P = \text{floor} [(T_{\max} - T_{\min}) / \Delta t]$ .  $\text{Floor}[\cdot]$  is a downward rounding operation. If the number of pulses is  $N$ , the computational complexity of the algorithm is  $O(NP)$ . Since  $N$  and  $P$  belong to the same order of magnitude, the overall time cost of running the algorithm is  $O(N^2)$ , which is similar to that of the PRI transform algorithm and the algorithm in [21].

## 4. Simulation and Discussion

In order to verify the performance of the algorithm proposed in this paper, *Precall* in [23,24] is used as a measure of the algorithm's performance in one snap in the presence of  $Q$  radar emitters, which is defined as follows:

$$precall = \frac{1}{Q} \sum_{i=1}^Q \frac{TP_i}{P_i} \quad (16)$$

where  $TP_i$  is the number of pulses for which the  $i$ th radar emitter is sorted out and  $P_i$  is the number of pulses that really exist.

To measure the overall sorting performance of the algorithm, the statistical probability of false alarm  $P_f$  and the probability of correct sorting  $P_d$  are used to measure the performance of the algorithm

$$P_f = \frac{1}{N_p} \sum_{i=1}^{N_p} \frac{Q_{si}}{Q_i} \quad (17)$$

$$P_d = \frac{1}{N_p} \sum_{i=1}^{N_p} \frac{Q_{di}}{Q_i} \quad (18)$$

where  $N_p$  is the total number of snap of the sorted signal sequence,  $Q_{si}$  is the number of radar emitters from the additional batch in the  $i$ th snap that are included in the sorting

result,  $Q_{di}$  is the number of radar emitters of the sorting result in the  $i$ th snap that satisfies Equation (17), and  $Q_i$  is the number of radar emitters that really exist in the  $i$ th snap.

The simulation experiment parameter settings are shown in Table 1.

**Table 1.** Signal parameters of radar emitters.

Emitter No.	PRI Value ( $\mu$ s)	Frame Period ( $\mu$ s)	Sub-PRIs ( $\mu$ s)	Noise Error (%)	Missing Rate (%)	Pulse Number
Radar 1	415	—	—	[0, 40]	[0, 40]	[5, 100]
Radar 2	—	—	$110 + 10\sin(2\pi n/5), n = 1, 2, \dots, 5$	[0, 40]	[0, 40]	[5, 100]
Radar 3	—	—	$80 + 2n, n = 1, 2, \dots, 6$	[0, 40]	[0, 40]	[5, 100]
Radar 4	—	367	119, 121, 127	[0, 40]	[0, 40]	[5, 100]
Radar 5	387	—	—	[0, 40]	[0, 40]	[5, 100]
Radar 6	—	—	$87 + 10\cos(2\pi n/12), n = 1, 2, \dots, 12$	[0, 40]	[0, 40]	[5, 100]
Radar 7	—	—	$91 + 3n, n \in [1, 5]; 124 - 3n, n \in [6, 10]$	[0, 40]	[0, 40]	[5, 100]
Radar 8	—	798	111, 131, 147, 119, 123, 167	[0, 40]	[0, 40]	[5, 100]

Note: “—” Indicates that no parameter setting.

#### 4.1. Experiment 1: Algorithm Validity Experiment

The radar emitters 1,2,3,4 in Table 1 are selected to form a signal environment: (1) a fixed PRI signal sequence with PRI of 415  $\mu$ s, and the TOA of the first pulse is 15  $\mu$ s; (2) a sinusoidal modulated signal sequence with PRI center value of 110  $\mu$ s, and the pattern of the single-frame is  $\sin(2\pi n/5)$  with  $n = 1, 2, \dots, 5$ , and the first pulse arrival time is 35  $\mu$ s; (3) the PRI start value is 80  $\mu$ s of the sliding PRI signal, the single-frame change pattern is  $2n$ , ( $n$  is the pulse number and  $n = 1, 2, \dots, 6$ , with a first pulse arrival time of 118  $\mu$ s); (4) a 3-staggered PRI signal sequence with a sub-PRI of [119  $\mu$ s 121  $\mu$ s 127  $\mu$ s], the first pulse arrival time is 91  $\mu$ s.

Figure 7 shows the congruence transform and detection results of the signal sequence in the signal environment of Experiment 1. From Figure 7a, it can be seen that the remainder histogram of the interleaved signal has a peak in the frame period in the periodic PRI signal, and the histogram of the remainder has a small value in the other values. The peak detection leads to Figure 7b, where the remainder histogram has peaks at frame periods of 367  $\mu$ s, 415  $\mu$ s, 500  $\mu$ s, and 522  $\mu$ s. The location of the peaks is consistent with the conclusion of Equation (10). It means that direct acquisition of the sub-PRI sequences is allowed, and the proposed periodic PRI signal sorting algorithm is efficient.

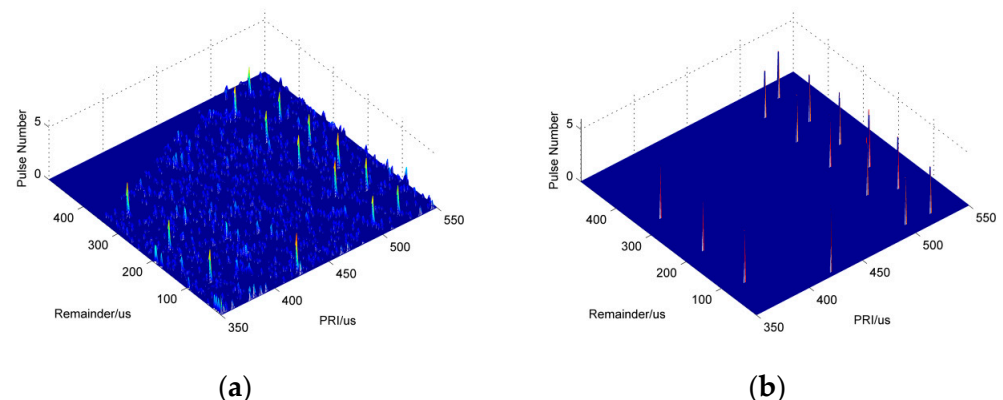


**Figure 7.** Algorithm processing results of this paper: (a) result of a congruence transform; (b) results after congruence transform detection.

#### 4.2. Experiment 2: Experiment on the Effect of the Number of Emitters on the Performance of the Algorithm

To verify the performance of the algorithm further, 100 times randomly selected 2, 3, 4, 5, 6, and 7 radar emitter signals in Table 1 are combined to form a sequence of overlapping

signals under different signal environments. Both the pulse loss ratio and the interference pulse ratio are set to 5%. The experiments are processed using the algorithm in [19], the algorithm in [21], and the algorithm of this paper, respectively. The  $P_{recall}$ ,  $P_f$ , and  $P_d$  of the algorithm under the conditions of different numbers of radar emitters are shown in Figure 8.

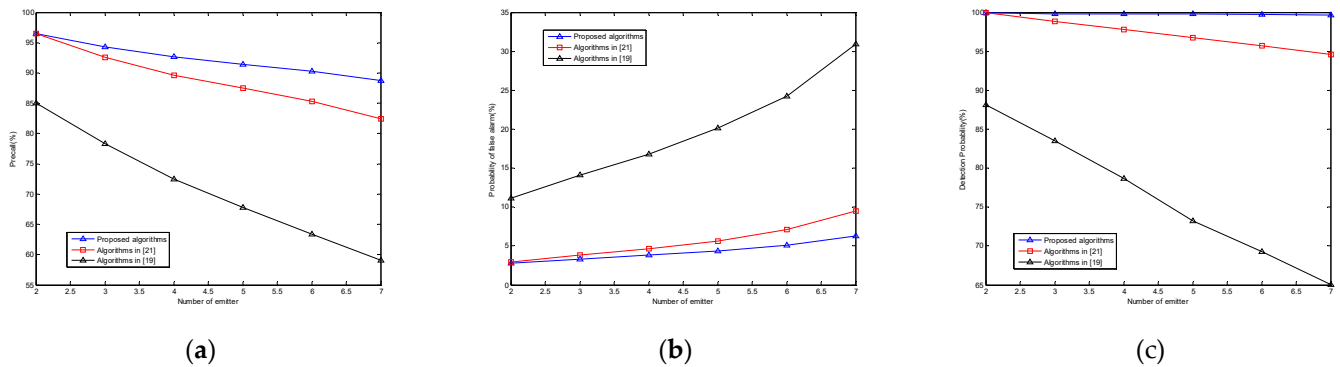


**Figure 8.** Sorting performance under different number of emitters: (a) average pulse recall; (b) probability of false alarm; (c) sorting probability of correct.

It can be seen from Figure 8a that, with the increase of the number of emitters, the pulse recall of the algorithm proposed in [19,21] and this paper decreases. In the case of 7 radar emitter signals being interleaved, the pulse recall of this paper's algorithm is about 89%, the pulse recall of the [21] algorithm is about 82%, and the pulse recall of the [19] algorithm is about 58%. Similarly, in Figure 8b,c, the algorithm in this paper outperforms those in [19,21] in terms of the probability of false alarms and the probability of detection.

As the number of emitters increases, the signals from the radar emitters interfere with each other, which affects the sorting performance of the algorithm, decreasing the algorithm's performance. The performance of the algorithm in [21] and the algorithm in this paper is closer when the number of emitters is small, and, as the number of emitters increases, the performance gap between the two algorithms increases. This is caused by the different performance of the two algorithms in adapting to the signals of radars 2, 3, 6, and 7. The algorithm in [19] has worse sorting performance for both periodic PRI signals and staggered PRI signals than the algorithms in this paper and in [21].

#### 4.3. Experiment 3: Experiment on the Impact of Pulse Loss Rate on Algorithm Performance

**Simulation setting:** In order to verify the performance of the algorithm in a complex electromagnetic environment, 100 experiments are performed. Emitter signals 2, 3, 4, 5, 6, and 7 in Table 1 are randomly selected and combined to form a sequence of overlapping signals under different signal environments. The loss rate takes the value of [10%, 20%, 30%, 40%], which is processed using the algorithms in [19,21] and this paper, respectively. Figure 9a–c show the performance of algorithms in this paper, [19,21] in terms of  $P_{recall}$ ,  $P_f$ , and  $P_d$ , respectively. Different colors and flags are used to distinguish the curves with different pulse loss rates.

In Figure 9, the performance of  $P_{recall}$ ,  $P_f$ , and  $P_d$  of the algorithm in [19,21] and this paper decreases with an increase in the number of emitters. With the increase in pulse loss rate, the performance of  $P_{recall}$ ,  $P_f$ , and  $P_d$  of the algorithm decreases in [19,21] and this paper. The performance of this paper's algorithm is better than that in [19,21], and the algorithm has good adaptability to pulse loss.

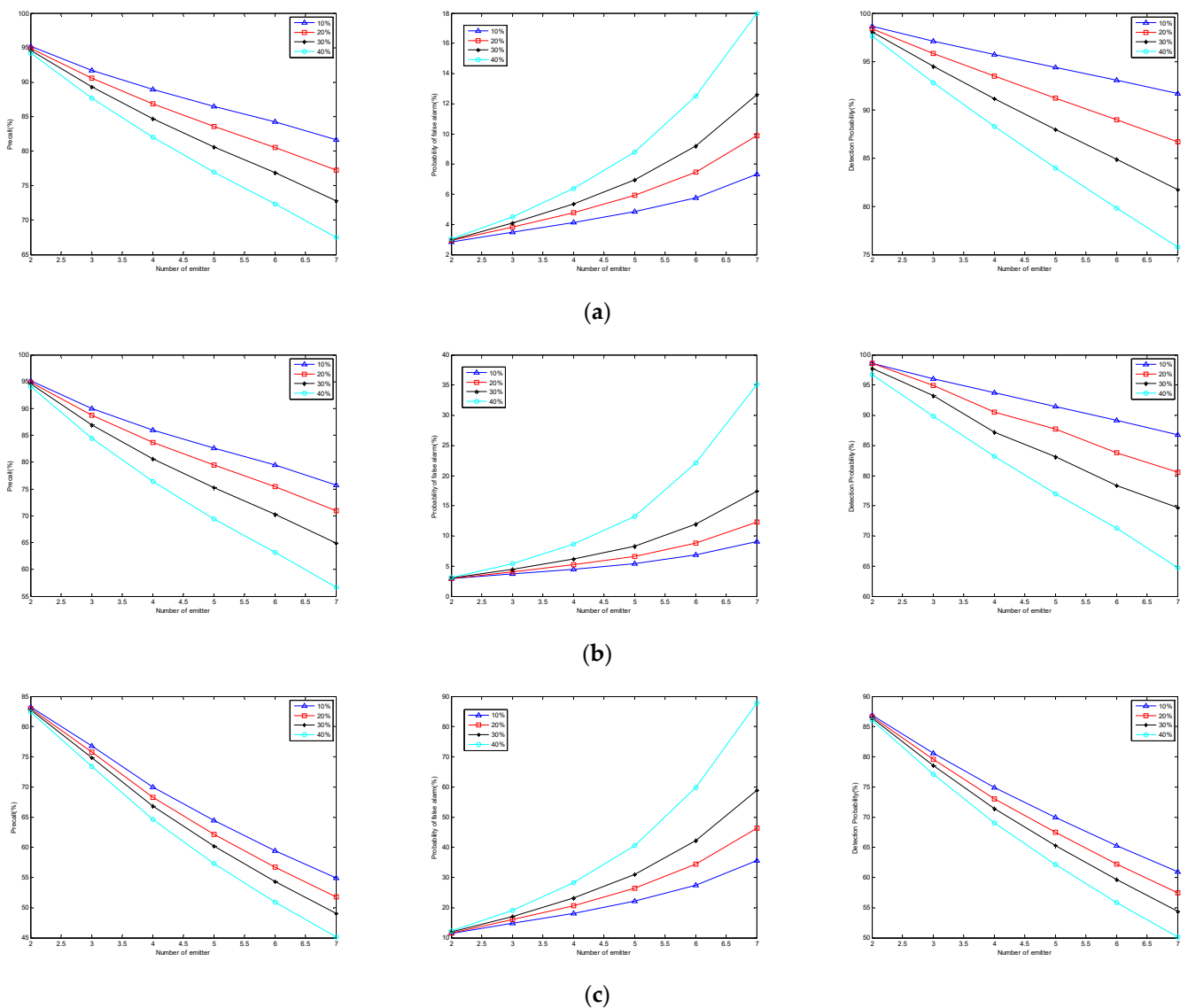


**Figure 9.** Impact of pulse loss rate on algorithm performance under different number of emitters: (a) sorting performance of the algorithm in this paper; (b) sorting performance of the algorithm in [21]; (c) sorting performance of the algorithm in [19].

#### 4.4. Experiment 4: Experiment on the Effect of Interference Pulse on Algorithm Performance

**Simulation setting:** To verify the performance of the algorithm in a complex electromagnetic environment, 100 experiments are performed. Emitter signals 2, 3, 4, 5, 6, and 7 in Table 1 are randomly selected and combined to form a sequence of overlapping signals under different signal environments. The interference pulse rate takes the value of [10%, 20%, 30%, 40%], which is processed using the algorithms in [19,21] and this paper, respectively. Figure 10a–c show the performance of algorithms in this paper, [19,21] in terms of  $P_{\text{recall}}$ ,  $P_f$ , and  $P_d$ , respectively. Different colors and flags are used to distinguish the curves with different interference pulse rates.

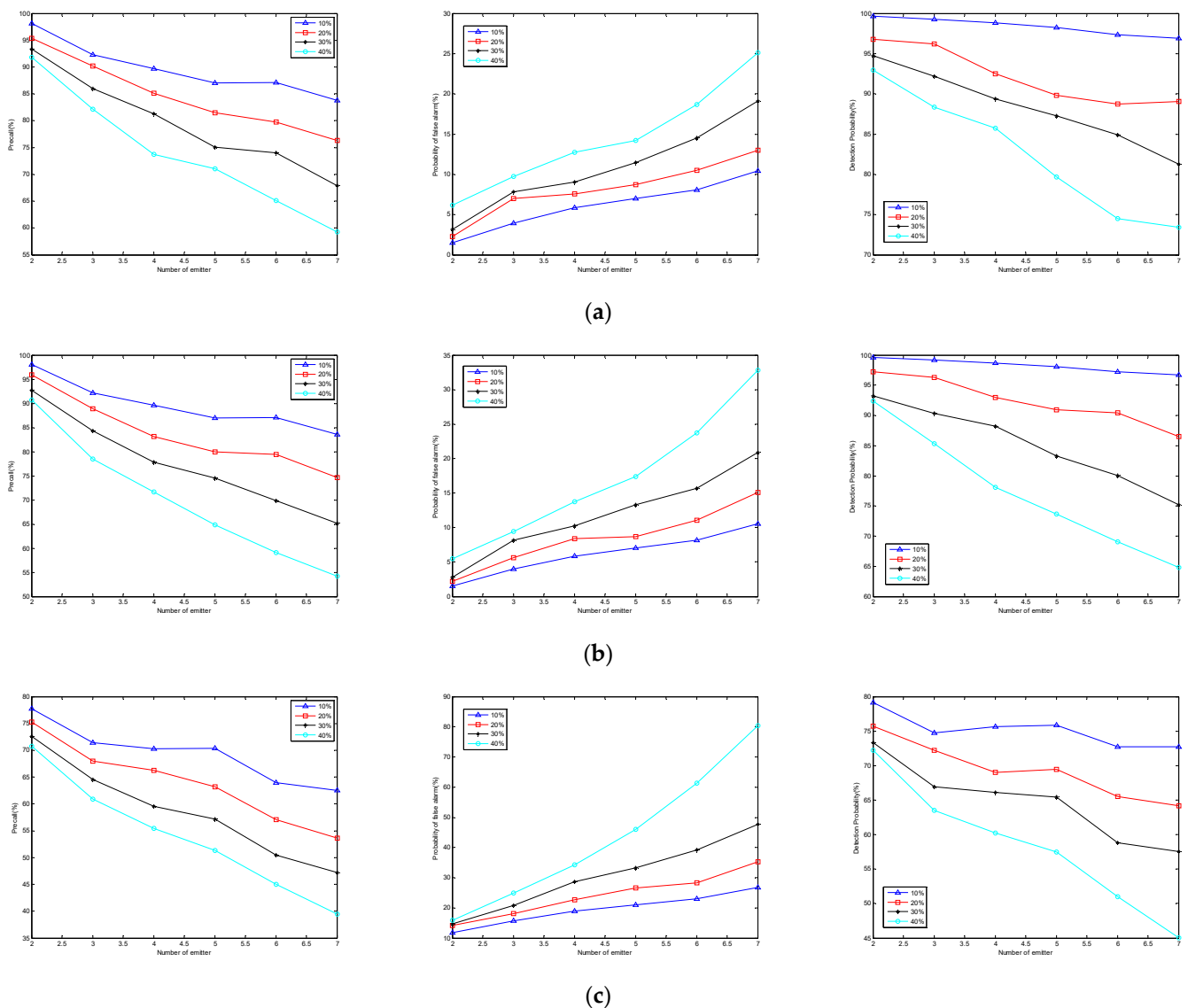


**Figure 10.** Impact of interference pulse ratio on algorithm performance under different number of emitters: (a) sorting performance of the algorithm in this paper; (b) sorting performance of the algorithm in [21]; (c) sorting performance of the algorithm in [19].

In Figure 10, the performance of  $P_{recall}$ ,  $P_f$ , and  $P_d$  of the algorithm in [19,21] and this paper decreases with an increase in the emitters' number. With an increase in the interference pulse rate, the performance of  $P_{recall}$ ,  $P_f$ , and  $P_d$  of the algorithm decreases in [19,21] and this paper. The performance of this paper's algorithm is better than that in [19,21], and the algorithm has good adaptability to interference pulses.

## 5. Conclusions

This paper discusses the application of congruence transform in periodic PRI signals sorting. Based on the analysis of the characteristics of periodic PRI signals, an improved algorithm is proposed. It can sort not only the staggered PRI signals, but also the periodic PRI signals. This improvement does not come at the expense of sacrificing the advantages of the algorithm in [21]. The results of the simulation experiments verify the above conclusions.

However, the computational complexity of this algorithm is  $\mathcal{O}(N^2)$ , which is not suitable for large-scale data processing, and the fast computation of this algorithm will be the focus of future research.

**Author Contributions:** Conceptualization, H.D. and Y.G.; methodology, H.D. and R.Z.; software, H.D. and H.W.; validation, H.D. and Y.G.; formal analysis, H.D. and R.Z.; investigation, H.D. and H.W.; resources, H.D. and Y.G.; data curation, H.D. and R.Z.; writing—original draft preparation, H.D.; visualization, Y.G.; supervision, R.Z. All authors have read and agreed to the published version of the manuscript.

**Funding:** This research received no external funding.

**Data Availability Statement:** The original contributions presented in the study are included in the article, further inquiries can be directed to the corresponding author.

**Conflicts of Interest:** The authors declare no conflicts of interest.

## References

1. Lang, P.; Fu, X.J.; Cui, Z.D.; Feng, C.; Chang, J.J. Subspace Decomposition Based Adaptive Density Peak Clustering for Radar Signals Sorting. *IEEE Signal Process. Lett.* **2022**, *29*, 424–428. [[CrossRef](#)]
2. Lang, P.; Fu, X.J.; Dong, J.; Yang, H.; Yang, J. A Novel Radar Signals Sorting Method via Residual Graph Convolutional Network. *IEEE Signal Process. Lett.* **2023**, *30*, 753–757. [[CrossRef](#)]
3. Liu, Z.M. Online pulse deinterleaving with finite automata. *IEEE Trans. Aerosp. Electron. Syst.* **2020**, *56*, 1139–1147. [[CrossRef](#)]
4. Manickchand, K.; Strydom, J.J.; Mishra, A.K. Comparative study of TOA based emitter deinterleaving and tracking algorithms. In Proceedings of the 2017 IEEE AFRICON, Cape Town, South Africa, 18–20 September 2017.
5. Zhao, S.Q.; Wang, W.H.; Zeng, D.G.; Chen, X.; Zhang, Z.; Xu, F.; Mao, X.; Liu, X. A novel aggregated multipath extreme gradient boosting approach for radar emitter classification. *IEEE Trans. Ind. Electron.* **2021**, *69*, 703–712. [[CrossRef](#)]
6. Guo, Q.; Teng, L.; Qi, L.; Ji, X.; Xiang, J. A Novel Radar Signals Sorting Method-Based Trajectory Features. *IEEE Access* **2019**, *7*, 171235–171245. [[CrossRef](#)]
7. Sui, J.P.; Liu, Z.; Liu, L.; Li, X. Progress in radar emitter signal deinterleaving. *J. Radars* **2022**, *11*, 418–433.
8. Mardia, H.K. New techniques for the deinterleaving of repetitive sequences. *IEE Proc. F Radar Signal Process.* **1989**, *136*, 149–154. [[CrossRef](#)]
9. Milojevic, D.J.; Popovic, B.M. Improved algorithm for the deinterleaving of radar pulses. *IEE Proc. F-Radar Signal Process.* **1992**, *139*, 98–104. [[CrossRef](#)]
10. Xie, M.; Zhao, C.; Zhao, Y.; Hu, D.; Wang, Z. A novel method for deinterleaving radar signals: First-order difference curve based on sorted TOA difference sequence. *IET Signal Process* **2022**, *17*, e12162. [[CrossRef](#)]
11. Guo, Q.; Huang, S.; Qi, L.A.; Wang, Y.N.; Kaliuzhnyi, M. A radar pulse train de-interleaving method for missing and short observations. *Eng. Electr. Electron.* **2023**, *141*, 104162.
12. Mahdavi, A.; Pezeshk, A.M. fast enhanced algorithm of PRI transform. In Proceedings of the 6th International Symposium on Parallel Computing in Electrical Engineering, Luton, UK, 3–7 April 2011; pp. 179–184.
13. Liu, Y.C.; Zhang, Q.Y. Improved method for deinterleaving radar signals and estimating PRI values. *IET Radar Sonar Navig.* **2018**, *12*, 506–514. [[CrossRef](#)]
14. Kocamış, M.B.; Torun, O.; Abaci, H.; Akdemir, Ş.B.; Yıldırım, A. Deinterleaving for radars with jitter and agile pulse repetition interval. In Proceedings of the 25th Signal Processing and Communications Applications Conference, Antalya, Turkey, 15–18 May 2017; pp. 1–4.
15. Liu, Z.M.; Kang, S.Q.; Chai, X.M. Automatic Pulse Repetition Pattern Reconstruction of Conventional Radars. *IET Radar Sonar Navig.* **2021**, *15*, 500–509. [[CrossRef](#)]
16. Kang, S.Q.; Liu, Z.M. Automatic reconstruction of regular radar pulse repetition patterns based on interleaved pulse train. *J. Signal Process.* **2021**, *37*, 2069–2076.
17. Wang, J.L.; Huang, Y.J. Stagger Pulse Repetition Interval Pulse Train Deinterleaving Algorithm Based on Sequence Association. *J. Electron. Inf. Technol.* **2021**, *43*, 1145–1153.
18. Tao, J.W.; Yang, C.Z.; Xu, C.W. Estimation of PRI Stagger in Case of Missing Observations. *IEEE Trans. Geosci. Remote Sens.* **2020**, *58*, 7982–8001. [[CrossRef](#)]
19. Cheng, W.H.; Zhang, Y.Y.; Dong, J.M.; Wang, C.; Liu, X.; Fang, G. An Enhanced Algorithm for De-interleaving Mixed Radar Signals. *IEEE Trans. Aerosp. Electron. Syst.* **2021**, *57*, 3927–3940. [[CrossRef](#)]
20. Tao, J.; Cui, W.; Chang, W. A fusion machine approach for pulse train deinterleaving. *Signal Image Video Process.* **2023**, *17*, 353–360. [[CrossRef](#)]
21. Dong, H.; Wang, X.; Qi, X.; Wang, C. An Algorithm for Sorting Staggered PRI Signals Based on the Congruence Transform. *Electronics* **2023**, *12*, 2888. [[CrossRef](#)]
22. Zhang, C.J.; Liu, Y.C.; Si, W.J. PRI modulation recognition and sequence search under small sample prerequisite. *J. Syst. Eng. Electron.* **2023**, *34*, 706–713. [[CrossRef](#)]

23. Kang, K.; Zhang, Y.X.; Guo, W.P. Key Radar Signal Sorting and Recognition Method Based on Clustering Combined with PRI Transform Algorithm. *J. Artif. Intell. Technol.* **2022**, *2*, 62–68. [[CrossRef](#)]
24. Ge, Z.P.; Sun, X.; Ren, W.J.; Chen, W.; Xu, G. Improved algorithm of radar pulse repetition interval deinter-leaving based on pulse correlation. *IEEE Access* **2019**, *7*, 30126–30134. [[CrossRef](#)]

**Disclaimer/Publisher’s Note:** The statements, opinions and data contained in all publications are solely those of the individual author(s) and contributor(s) and not of MDPI and/or the editor(s). MDPI and/or the editor(s) disclaim responsibility for any injury to people or property resulting from any ideas, methods, instructions or products referred to in the content.